Journal of Integrative Agriculture 2026, 25(9): 3775–3785

Available online at ScienceDirect

Journal of Integrative Agriculture

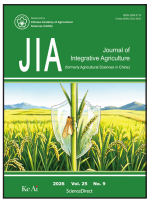

RESEARCH ARTICLE

Sex-specific and functional differentiation between OR23h and OR109d in aggregation pheromone detection in *Riptortus pedestris*

Xiaotong Zhang[1, 2, 3], Jiahang Wei[2], Xuanpu Luan[2], Ian W. Keesey[5], Xin Chen[4], Qi Yan[1, 2], Shuanglin Dong[1, 2#], Jin Zhang[1, 2, 3#]

[1] *Sanya Institute, Nanjing Agricultural University, Nanjing 210095, China*
[2] *State Key Laboratory of Agricultural and Forestry Biosecurity, College of Plant Protection, Nanjing Agricultural University, Nanjing 210095, China*
[3] *Key Laboratory of Soybean Disease and Pest Control of Ministry of Agriculture and Rural Affairs, Nanjing Agricultural University, Nanjing 210095, China*
[4] *Jiangsu Key Laboratory for Horticultural Crop Genetic Improvement/Institute of Industrial Crops, Jiangsu Academy of Agricultural Sciences, Nanjing 210014, China*
[5] *School of Biological Sciences, University of Nebraska — Lincoln (UNL), Lincoln 68588, USA*

Highlights

- *Riptortus pedestris* detects aggregation pheromones *via* its distiflagellum.
- OR23h is broadly tuned to three structurally similar components, E2HE2H, E2HZ3H, and E2HH, whereas the male-biased OR109d is narrowly tuned to E2HE2H.
- Dual RNAi treatment demonstrated that OR23h and OR109d collectively mediate the response to the primary component, E2HE2H.

Abstract

The bean bug, *Riptortus pedestris*, is a major pest of soybeans in East Asian countries. Male-released aggregation pheromones attract both adults and nymphs, offering potential for eco-friendly pest control. However, the molecular mechanisms underlying the detection of the aggregation pheromones remain unclear. In the present study, functional analysis using the *Xenopus* oocyte expression system demonstrated that two ORs (OR23h and OR109d) were responsible for sensing aggregation pheromones, with the primary component (E)-2-hexenyl (E)-2-hexenoate (E2HE2H) being shared by the two ORs. Further quantitative PCR (qPCR) profiling indicated that *OR109d* was expressed only in male antennae, while *OR23h* was expressed in both sexes at similar levels. RNA interference (RNAi) assays demonstrated that ds*OR23h*-treatment significantly reduced the electroantennographic (EAG) response of (*E*)-2-hexenyl (*Z*)-3-hexenoate (E2HZ3H) in both sexes. Furthermore, simultaneous RNAi knockdown of the two ORs significantly reduced the male EAG response to E2HE2H and abolished male attraction to this compound. These results were consistent with the sex expression profile, demonstrating the sex and functional differentiation between the two ORs. Taken together, this study characterizes the ORs responsible for chemical perception and the associated aggregation behaviors driven by these pheromones. Thus, this study enhances our understanding of olfactory signaling in a hemipteran insect and contributes to the knowledge required for improved pest management.

Keywords: odorant receptors, *Xenopus* oocyte expression and two-electrode voltage clamp, RNA interference, synergism, EAG response, behavioral preference

1. Introduction

Pheromones are chemical substances released by animals that influence the behavior or physiology of conspecifics (Karlson and Lascher 1959). In insects, pheromone communication plays critical roles in food and host location, alarm signaling, aggregation, and reproduction (Vickers 2017; Liu *et al.* 2025; Sun *et al.* 2025). These functions rely on a chemically diverse array of volatile and non-volatile signals.

Received 8 August 2025; Received in revised form 24 Spetember 2025; Accepted 9 October 2025; Available online 7 November 2025
#Correspondence Jin Zhang, E-mail: jinzhang001@njau.edu.cn; Shuanglin Dong, E-mail: sldong@njau.edu.cn

doi: 10.1016/j.jia.2025.11.009

Typically, volatile pheromones are detected by olfactory sensilla on the antennae, while non-volatile pheromones are perceived through gustatory sensilla located mainly on the proboscis and legs (Hansson and Stensmyr 2011; Yew and Chung 2015). For olfaction, when pheromone molecules enter a sensillum through pores in the cuticle, they interact with sensory proteins, including chemosensory proteins (CSPs), odorant binding proteins (OBPs), ionotropic receptors (IRs) and odorant receptors (ORs). Among these proteins, ORs encoded by highly diverse gene families and characterized by a seven-transmembrane domain structure, play a key role in the specificity and sensitivity of the olfaction (Hallem *et al.* 2006; Hallem and Carlson 2006; Hansson and Stensmyr 2011; Leal 2013; Sims *et al.* 2022).

Aggregation pheromones, typically comprising blends of multiple volatile compounds, serve as cues that attract conspecifics and promote congregation for essential activities such as foraging, sheltering, mating and other social behavior (Wertheim *et al.* 2005, 2006). Well-characterized in diverse taxa including locusts, bark beetles, and cockroaches (Guo *et al.* 2020; Tateishi *et al.* 2020; Yuvaraj *et al.* 2021), aggregation pheromones are critical for insect survival and reproduction and provide valuable insights into behavioral mechanisms and potential pest management strategies (Guo X J *et al.* 2023; Kong *et al.* 2025). In the bean bug *Riptortus pedestris* (Hemiptera: Alydidae), the aggregation pheromone consists of a five-component blend: tetradecyl isobutyrate (14:iBu), octadecyl isobutyrate (18:Bu), (*E*)-2-hexenyl (*Z*)-3-hexenoate (E2HZ3H), (*E*)-2-hexenyl (*E*)-2-hexenoate (E2HE2H), and (*E*)-2-hexenyl hexanoate (E2HH) (Leal and Kadosawa 1992; Leal *et al.* 1995; Yasuda *et al.* 2007a, b). These compounds attract both nymphs and adult conspecifics of both sexes (Numata *et al.* 1990; Leal *et al.* 1995). However, its composition varies with age, photoperiod, nutritional status, and food source (Morishima *et al.* 2005; Mizutani *et al.* 2008a, b; Huh *et al.* 2009; Huh and Park 2010), underscoring the functional complexity and plasticity of these chemical signals.

Among the five components, 14:iBu is essential for aggregation (Mizutani *et al.* 1997), whereas E2HZ3H and E2HE2H enhance its attractiveness (Endo *et al.* 2005; Huh *et al.* 2005). The functions of the remaining two components, 18:iBu and E2HH, are not fully characterized. E2HH, first identified as an alarm pheromone in both sexes of *R. pedestris*, triggers dispersive behavior under controlled conditions (Leal and Kadosawa 1992). Field experiments have produced conflicting results. While some studies suggested that 18:iBu or E2HH may enhance the attractiveness of 14:iBu (Yasuda *et al.* 2007a, b), others showed that combining the aggregation pheromone with E2HH significantly reduced trap efficacy (Rahman and Lim 2017). Although aggregation pheromone traps are typically effective for pest monitoring and mass capture, they perform poorly in *R. pedestris* (Rahman *et al.* 2018). Elucidating the underlying olfactory molecular mechanisms could inform the design of behaviorally active compounds for pest monitoring or management. Although E2HZ3H binds to chemosensory protein CSP12, the specific ORs responsible for detecting aggregation pheromones in *R. pedestris* remain unidentified. This knowledge gap impedes the development of effective control strategies, including trapping systems (Tabuchi *et al.* 2005; Rahman *et al.* 2018).

This study aimed to identify ORs mediating aggregation pheromone detection in *R. pedestris* and elucidate perception mechanisms. We first localized pheromone perception to the antennal distiflagellum using electroantennography (EAG). Candidate ORs were screened *via* comparative transcriptomics based on distiflagellum-biased expression. Functional validation employed *Xenopus* oocyte expression coupled with two-electrode voltage clamp (XOE-TEVC) and RNA interference (RNAi). Finally, phylogenetic analysis and XOE-TEVC were integrated to identify additional pheromone-responsive ORs and examine their ligand specificity and combinatorial interactions. This comprehensive approach not only identifies key ORs underlying aggregation pheromone perception but also deciphers the combinatorial coding strategies governing olfactory processing of single pheromone components.

2. Materials and methods

2.1. Insect rearing

Samples of *R. pedestris* used in this study, originally collected from Baima Base at Nanjing Agricultural University, Nanjing, China, were reared in the laboratory on soybeans (both seeds and living plants) under controlled conditions of (25±1)°C, (60±10)% relative humidity, and 14 h light:10 h dark photoperiod. Upon adult emergence, males and females were separated into individual containers for subsequent experiments.

2.2. EAG recordings

The EAG responses were measured in 7-day-old virgin male and female *R. pedestris*. Aggregation pheromone doses (0.001, 0.01, 0.1, 1, 10, 100, 500, and 1,000 μg) were prepared in hexane (solvent control). Filter paper strips (2.5 cm×0.8 cm) with either solvent control or pheromone solutions were placed in clean Pasteur tubes as odorant sources. EAG recordings followed previously established procedures (Liu *et al.* 2020; Zhang *et al.* 2024) and were conducted using an IDAC 4 Data Acquisition Controller with a CS-55 Stimulus Airflow Generator (Syntech, Germany) or an AUTO SPIKE IDAC-2/3 with a CS-05 Stimulus Airflow Generator (Syntech, Germany) (the latter was used only in dose-response tests with 14:iBu, 18:iBu, E2HE2H, E2HZ3H and E2HH). A 30 s interval between stimuli was maintained to ensure antennal recovery. The pheromone component E2HZ3H (purity>94%) was generously provided by Pherobio Technology Co., Ltd., China, while other components (purity>95%) were synthesized in Laboratory of Natural Products and Pesticide Chemistry, College of Plant Protection, Nanjing Agricultural University, China.

2.3. Transcriptome sequencing and analysis

Total RNA was extracted from the distiflagellum and other part of the antennae of 50 adults (older than 5 days) in a 1:1 sex ratio using TsingZol reagent (Tsingke, China) in accordance with the manufacturer's protocol. RNA integrity

and concentration were evaluated using 1% agarose gel electrophoresis and a NanoDrop 2000 spectrophotometer (Thermo Scientific, USA). Subsequent cDNA synthesis and transcriptome sequencing were performed by NovoGene Bioinformatics Technology Co., Ltd., China on an Illumina Novaseq 6000 PE150 platform. Clean reads were aligned to the reference genome (accession no. GWHBAZI00000000), and gene expression levels were quantified as fragments per kilobase of exon model per million mapped reads (FPKM). Differential expression analysis was conducted using the DESeq2 package (Love *et al.* 2014) with *P*-values adjusted (padj) *via* the Benjamini-Hochberg method to control the false discovery rate. ORs with the padj<0.05 and $|\log_2$(fold change)|>1 were classified as differentially expressed genes (DEGs).

2.4. Functional assays of differentially and highly expressed ORs using XOE-TEVC

Fifteen highly expressed DEG ORs were amplified by PCR with primers containing homologous sequences of the pGH19 plasmid and *Eco*RI or *Xba*I restriction sites (Appendix A). The products were cloned into the pGH19 expression vector using the ClonExpress One Step Cloning Kit (Vazyme, China). Recombinant plasmids were verified by sequencing and subsequently linearized using the FastDigest enzyme NotI/NdeI/NheI (Thermo Fisher, USA). The linearized plasmids served as templates for cRNA synthesis with the T7 High Yield RNA Transcription Kit (Vazyme, China), and the resulting cRNAs were diluted to 2,000 ng μL^{-1} in nuclease-free water and stored at –80°C.

Xenopus oocyte pretreatment, microinjection, and culture followed established protocols (Liu *et al.* 2020; Guo J M *et al.* 2023). A ligand-specific receptor (ORx) and a co-receptor protein (Orco) cRNAs were mixed in a 1:1 ratio, and 27.6 nL of the mixture was injected into mature, healthy oocytes. After 4 days of incubation, odor-induced currents were recorded using an Axoclamp 900A Microelectrode Amplifier (AutoMate Scientific Inc., USA) with TEVC at a holding potential of –80 mV. Currents were digitized *via* the Axon Digidata 1440A System (AutoMate Scientific, Inc., USA).

Odorants stock solutions were prepared at a concentration of 10^{-1} mol L^{-1} in dimethyl sulfoxide (DMSO). VUAA1 and 14 odorant mixtures, consisting of 132 common plant volatiles and 5 aggregation pheromones (Appendix B), were prepared by diluting each odorant to 10^{-4} mol L^{-1} in standard oocyte saline (SOS) buffer. For mixtures eliciting current responses, individual odorants were subsequently tested. Dose-response assays were conducted for odorants that induced the highest responses. Each odorant mixture or individual odorant was tested on 8 to 12 oocytes. For OR23, OR23x, and OR23c, only pheromones and structurally similar ester host odors were tested.

2.5. Construction of phylogenetic tree

A phylogenetic tree was constructed using amino acid sequences of total 519 ORs, including 164 ORs (>350 amino acids) from *R. pedestris* and 355 ORs from additional insect species, such as *Halyomorpha halys* (Hhal), *Apolygus lucorum* (Aluc), *Yemma signatus* (Ysig), *Tropidothorax elegans* (Tele), along with Orco sequences from *Diaphorina citri* (Dcit), *Cimex lectularius* (Clec), *Acyrthosiphon pisum* (Apis), and *Nilaparvata lugens* (Nlug). Sequence alignment was performed in MEGA X using the MUSCLE method with default parameters. The maximum-likelihood tree was constructed with FastTree v. 2.1.11, and bootstrap support values were computed using SH-like approximation with 1,000 replicates. The resulting tree was visualized and edited in iTOL (https://itol.embl.de/), and the Orco lineage was used to root the tree.

2.6. Expression profiles by quantitative PCR (qPCR)

The experimental procedures in this section are identical to those described in our previous study (Zhang *et al.* 2024). Briefly, the antennae from 1st to 5th instar nymphs and tissues from 7-day-old male and female adults were collected for qPCR analysis. First-strand cDNA was synthesized from 1 μg of total RNA extracted from various tissues using HiScript III RT SuperMix (Vazyme, China) to serve as the template for subsequent qPCR analysis. qPCR was performed on the QuantStudio™ 6 Flex Real-Time PCR System (Applied Biosystems, USA) in a 10 μL reaction volume using ChamQ Universal SYBR qPCR Master Mix (Vazyme, China), according to the manufacturer's instructions. The reaction conditions were as follows: 95°C for 30 s, followed by 40 cycles of 95°C for 5 s and 60°C for 34 s. Elongation factor 1 alpha (*EF1-α*) and *β-tubulin* were used as references to normalize the target gene expression. Gene expression levels were analyzed using the $2^{-\Delta\Delta CT}$ method.

2.7. RNAi assays

Orco, *OR23h*, *OR109d*, and green fluorescent protein (*GFP*, as a control) were amplified using primers with T7 promoter sequences (Appendix A). PCR products were purified using the FastPure Gel DNA Extraction Mini Kit (Vazyme, China) and used as templates for *in vitro* double-stranded RNAs (dsRNA) synthesis with the T7 RiboMAX™ Express RNAi System (Promega, USA). Fifth instar nymphs were anesthetized with carbon dioxide for 6–8 s, and approximately 4 μg of dsRNA was injected into the antennal socket using the MICRO4™ (WPI, USA). For single-gene interference, 4 μg of dsRNA was used per gene; for simultaneous interference, 2 μg of each dsRNA was mixed in a 1:1 ratio for both genes. After injection, insects were fed with water and soybean seeds. RNAi efficiency was assessed on days 3, 5, and 7 post-injection for *Orco*, and on day 7 for *OR23h* and *OR109d* using qPCR, as described above. Only living and healthy adult insects were selected for EAG recordings and behavioral assays.

2.8. Behavioral assays

The behavioral response of *R. pedestris* adults to aggregation pheromones was tested using a three-chamber olfactometer (Appendix C). The two side chambers (6.8 L each) contained a rubber lure placed in a Petri dish with water-saturated cotton: one with 300 μg of pheromone and the other with equal volumes of hexane as a control. The central chamber

(7.6 L) was left empty. Lures were prepared 1 h before the test and allowed to air-dry. Insects, starved for 24 h starting on day 6 post-injection, were selected and placed in the middle chamber for 12 h. Males and females were tested separately. If an insect entered one of the side chambers and stayed, it was considered to have "made a choice"; otherwise, it was recorded as "no choice." Each trial was repeated 8 times with 20 individuals per trial. Airflow (0.4 L min^{-1}) was filtered through activated charcoal, entering the side chambers and exiting through the middle chamber.

2.9. Data analysis

Statistical analyses were performed using GraphPad Prism 8 (GraphPad Software, USA). ANOVA followed by Fisher's LSD was used to compare gene expression levels or EAG responses across multiple groups, while Student's *t*-test was applied to compare differences between two groups in behavioral assays. Statistical significance was set at $P<0.05$.

3. Results

3.1. EAG responses of *R. pedestris* to aggregation pheromones

EAG responses of male and female adults to the five aggregation pheromone components at varying dosages were measured (Fig. 1-A). Results showed that 18:iBu failed to induce a detectable response in either sex at any tested dosage. In contrast, the remaining four components elicited significant dose-dependent responses, with no statistically significant differences observed between males and females. Among these active components, E2HE2H elicited the strongest EAG response.

To test whether the distiflagellum serves as the primary segment sensitive to aggregation pheromones, EAG responses were compared between intact adult antennae and those between adult antennae with or without the distiflagellum. Removal of the distiflagellum (Fig. 1-B) resulted in a substantial reduction in responses to the four components, with response magnitudes comparable to those of the solvent control (n=6–10, $P<0.001$) (Fig. 1-C). These findings confirm that the distiflagellum is the primary site for detecting aggregation pheromones.

3.2. Screening and *in vitro* functional characterization of aggregation pheromone-detecting ORs

To determine whether ORs or other olfactory receptors (e.g., ionotropic receptors, IRs) mediate the detection of aggregation pheromones, we employed RNAi to silence the olfactory co-receptor Orco. qPCR analysis confirmed significant reductions in *Orco* transcript levels by 81, 92, and 88% at 3, 5, and 7 days post-injection, respectively (Appendix D). EAG assays revealed that ds*Orco*-treated adults exhibited a 70% reduction in antennal responses to the four active pheromone components compared to controls at day 7 (Appendix D). These results underscore the critical role of ORs in pheromone detection.

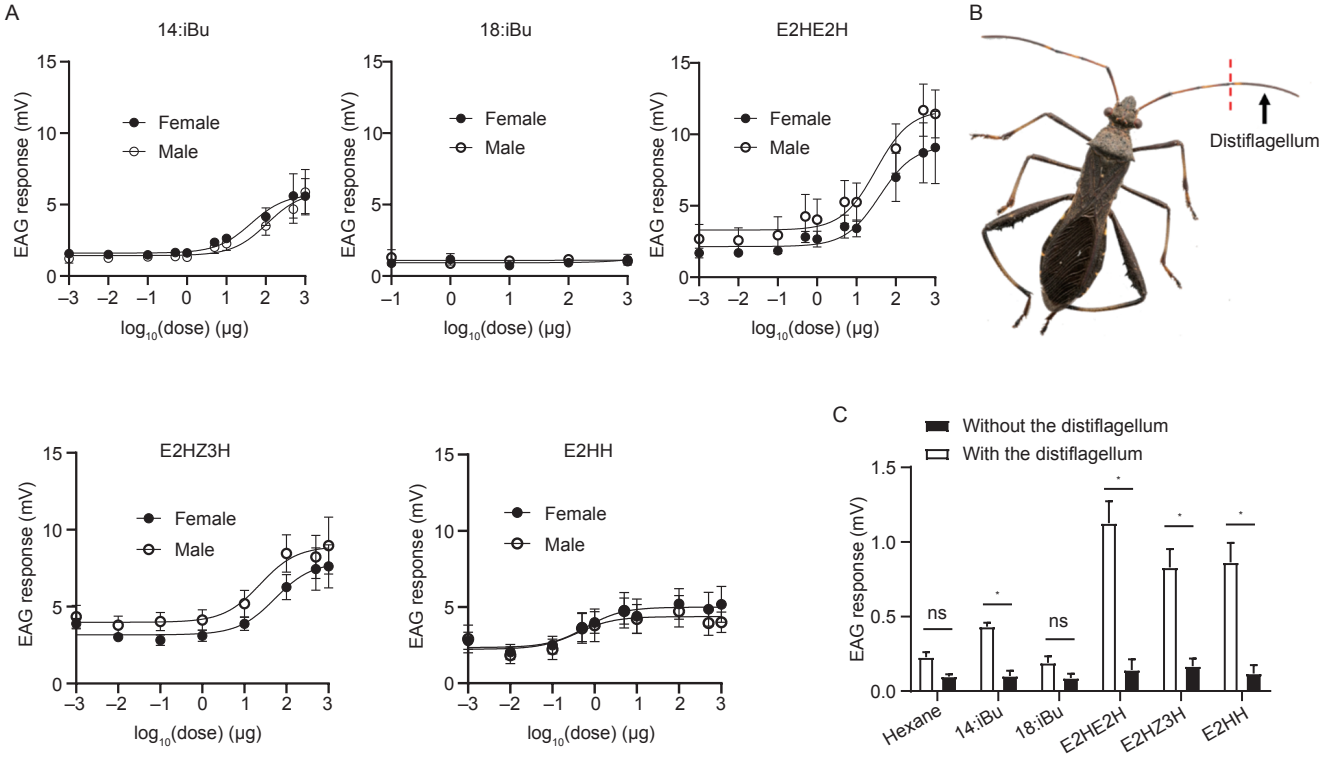

Fig. 1 Electroantennographic (EAG) response of adult *Riptortus pedestris* to five aggregation pheromones. A, EAG dose-responses to aggregation pheromones in both sexes. No significant difference was found between males and females (Student's *t*-test, $P<0.05$). Data represent mean±SEM (n=6–10). B, adult *R. pedestris* and its antennae, highlighting the distiflagellum. C, responses of antennae with and without the distiflagellum. Asterisks indicate significant differences between antennae with and without the distiflagellum (Student's *t*-test; *, $P<0.05$), while 'ns' indicates no significant difference; data represent mean±SEM (n=5).

To identify specific ORs involved in pheromone detection, we performed transcriptome sequencing on the distiflagellum and other part of the antennae. Among 277 detected ORs, approximately two-thirds (197 DEG ORs) were found to be primarily expressed in the distiflagellum. We prioritized the 15 most highly expressed ORs (Appendix E) for functional characterization using the *Xenopus* oocyte heterologous expression system. Of the 15 ORs tested, only OR101, OR23h and OR109d exhibited responses to the pheromone mixture (10^{-4} mol L^{-1}). Notably, OR101 exhibited an unusual outward current (Appendix F), whereas OR23h and OR109d generated normal inward currents (Figs. 2-A and 3-A). Further tests with four individual pheromone components revealed that the latter two ORs displayed different ligand profiles. OR23h strongly responded to E2HZ3H (EC_{50}=3.411×10^{-5} mol L^{-1}) and weakly to E2HE2H and E2HH (Fig. 2-B and C), while OR109d specifically responded to E2HE2H (Fig. 3-B and C). Oocytes expressing the remaining 12 ORs did not respond to either VUAA1 (an agonist of Orco) or the tested mixture, confirming their non-involvement in pheromone detection.

3.3. Expression profiles and *in vivo* functional validation of *OR23h* and *OR109d* by RNAi

To explore the functional significance of the two ORs across

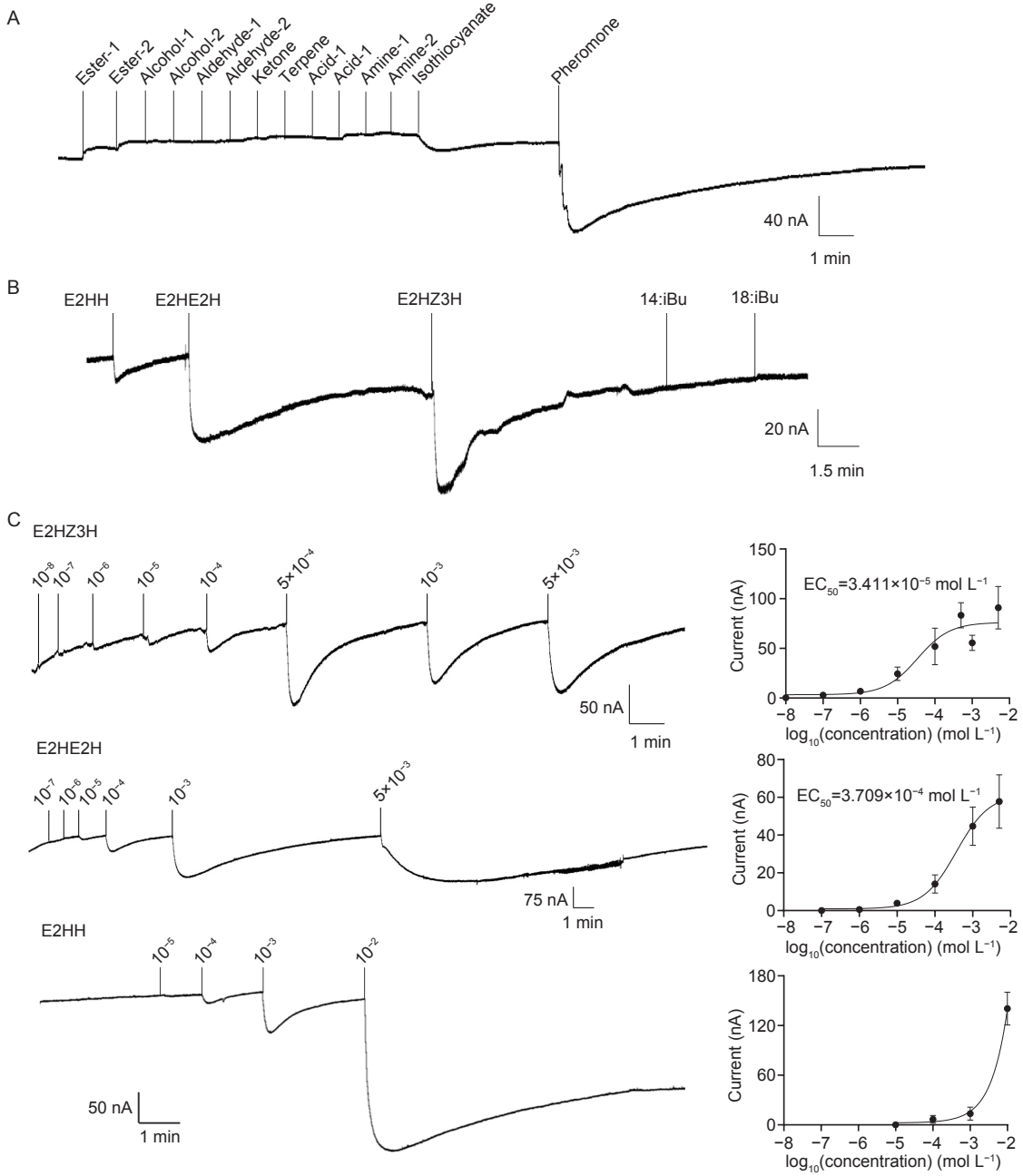

Fig. 2 Two-electrode voltage clamp recording of *Xenopus* oocytes expressing *OR23h/Orco*. A, responses to 14 odor mixtures (10^{-4} mol L^{-1} for each odor, see Appendix B for more details). B, responses to the five individual aggregation pheromones (5×10^{-4} mol L^{-1}). C, dose responses induced by E2HZ3H, E2HE2H and E2HH. Data represent mean±SEM (*n*=9–11).

nymphs and adults, we quantified the expression profiles of *OR23h* and *OR109d* using qPCR (Fig. 4). *OR23h* was highly expressed in adult antennae but weakly in nymph antennae, with no significant differences observed between sexes. In contrast, *OR109d* was specifically expressed in the antennae of adult males.

To confirm the *in vivo* roles of OR23h and OR109d in pheromone detection, we performed RNAi assays in adults, knocking down each gene individually (OR109d was not targeted in females due to its male-specific expression) and in combination. In females, seven days post-injection, *OR23h* knockdown alone reduced its expression by 78.6% (Fig. 5-A, n=8, P=0.0096). This resulted in a significant decrease in EAG response to E2HZ3H, E2HE2H, and E2HH by 44.4% (n=14, P=0.0028), 40.0% (n=13–14, P=0.0327), and 44.3% (n=14, P=0.0327) respectively, relative to the dsGFP control (Fig. 5-B), and eliminated the female preference for E2HZ3H (n=8, P=0.9176) (Fig. 5-C).

In males, *OR23h* knockdown alone significantly reduced gene expression by 92.3% (n=4, P=0.031) (Fig. 5-A), which led to a 33.2% (n=9–10, P=0.0043) decrease in EAG response to its primary ligand E2HZ3H without affecting

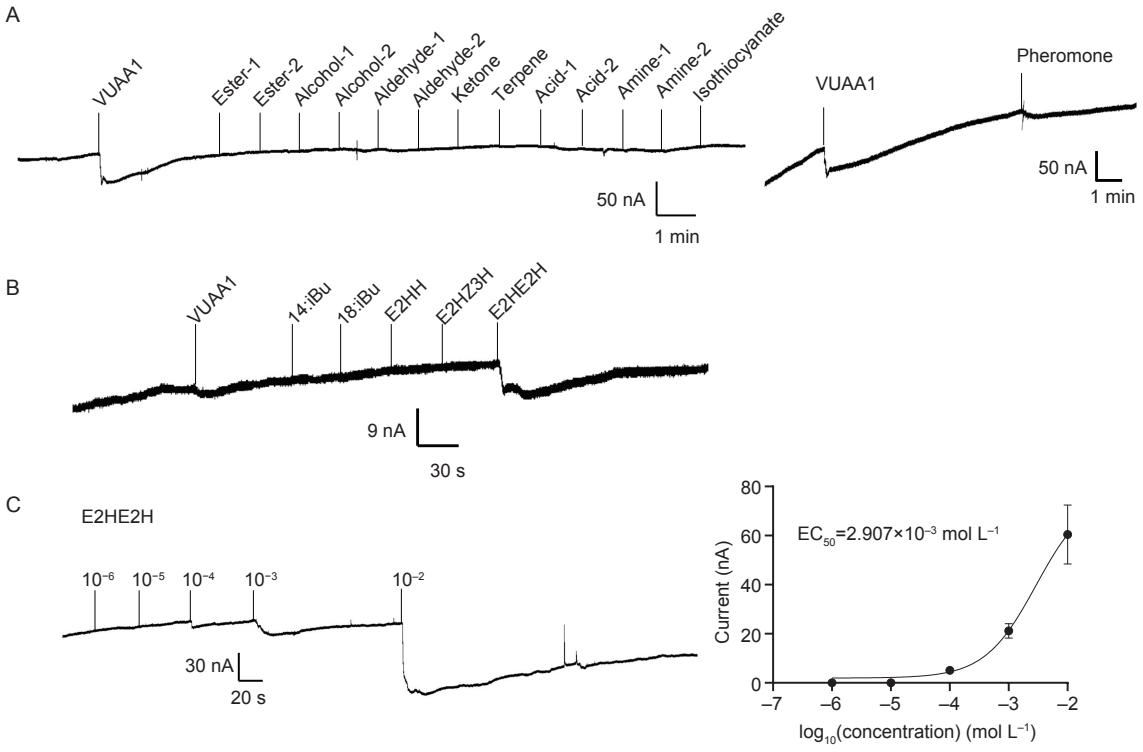

Fig. 3 Two-electrode voltage clamp recording of *Xenopus* oocytes expressing *OR109d/Orco*. A, responses to VUAA1 and 14 odor mixtures (10^{-4} mol L^{-1} for each odor, see Appendix B for more details). B, responses to individual odor in the mixture of pheromones (5×10^{-4} mol L^{-1}). C, dose responses induced by E2HE2H. Data represent mean±SEM (n=8–12). E2HH or E2HZ3H was not used in the concentration-response assay due to the absence of electrophysiological responses at 5×10^{-4} mol L^{-1}.

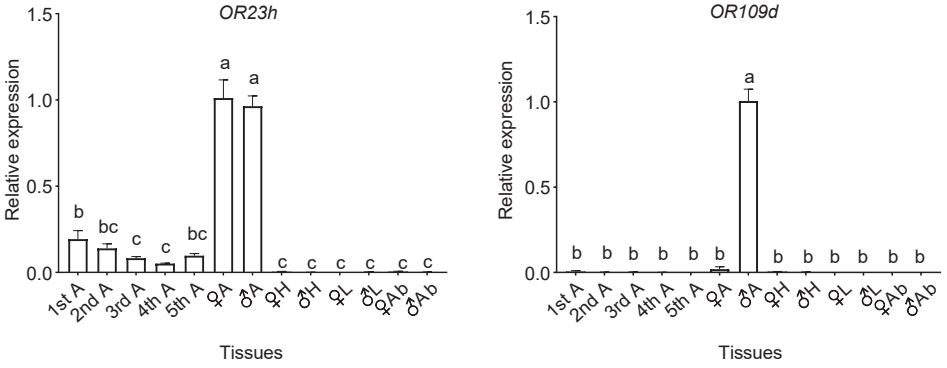

Fig. 4 Expression profile of *OR23h* and *OR109d*, regarding antennae of nymphs at different instars and different tissues of male and female adults. 1st–5th, nymph instar; A, antennae; H, heads without antennae; L, legs; Ab, the last two segment of the abdomen. Data represent mean±SEM (n=3). Different letters above the error bars represent significant difference between tissues (one-way ANOVA followed by the LSD test, P<0.05).

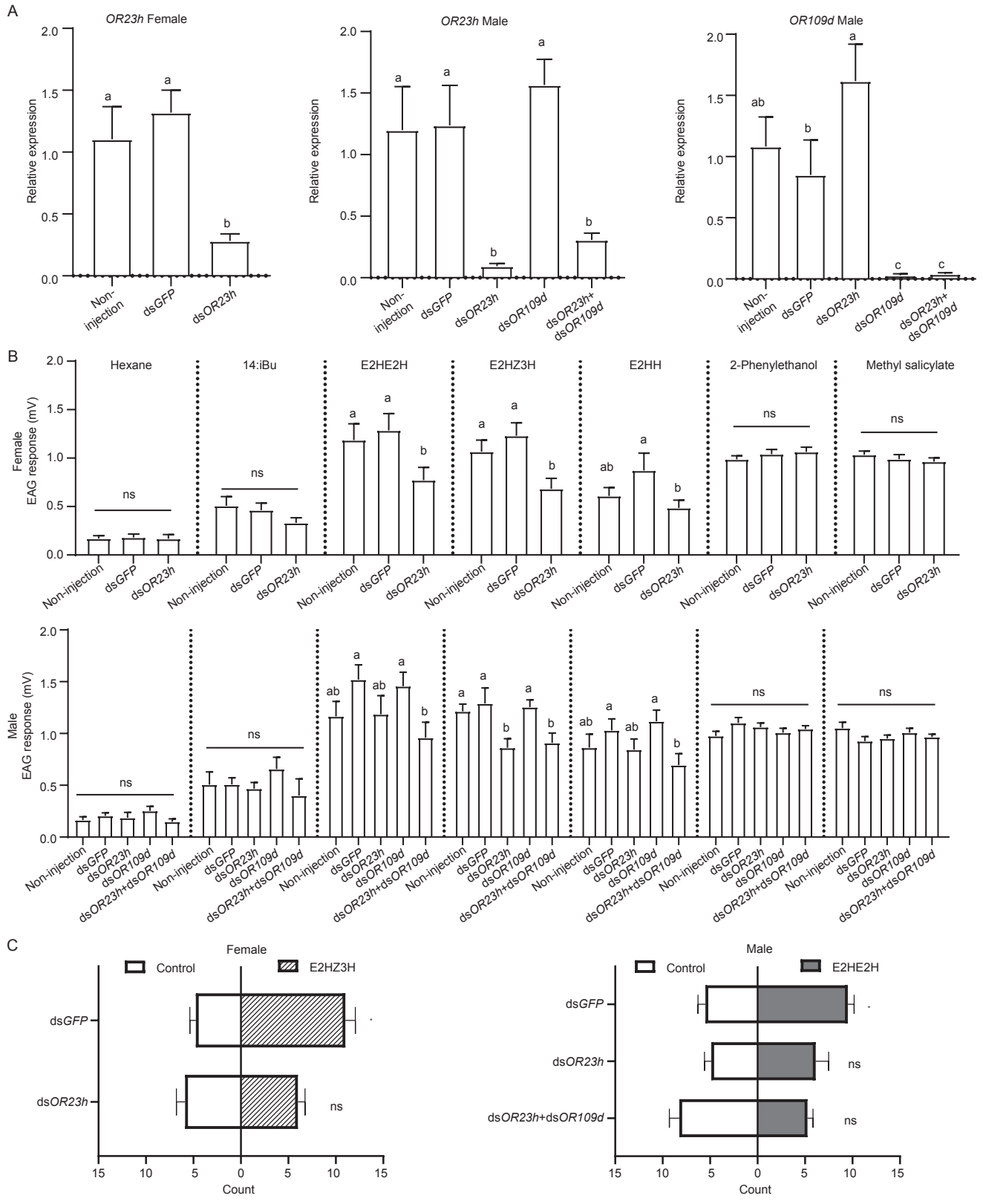

Fig. 5 Effect of RNA interference (RNAi) targeting *OR23h* and *OR109d* on electroantennographic (EAG) and behavioral response to aggregation pheromones. A, RNAi efficiency for *OR23h* in females and males, and for *OR109d* in males. Data represent mean±SEM (*n*=4–8). Different letters indicate significant differences in gene expressions among different treatments (one-way ANOVA followed by the LSD test, *P*<0.05). B, EAG responses of females and males with and without RNAi treatment. Data represents mean±SEM (*n*=7–15). Different letters above the error bars indicate significant differences to the same odor among different treatments (one-way ANOVA followed by LSD test, *P*<0.05), while 'ns' indicates no significant difference among treatments. C, behavioral response of males and females with different treatment in the three-chamber olfactometer (see Appendix C for more details). Data represent mean±SEM (*n*=8). Asterisks indicate significant differences in the number of bugs between the hexane (control) and pheromone treatments (Student's *t*-test, *, *P*<0.05), while 'ns' indicates no significant difference.

responses to E2HE2H (n=9, P=0.1220) or E2HH (n=9–10, P=0.2586) (Fig. 5-B). *OR109d* knockdown alone reduced its expression by 96.7% (n=5, P=0.0076) (Fig. 5-A) but had no impact on EAG responses to any pheromone components (Fig. 5-B). Co-knockdown of *OR23h* and *OR109d* reduced their expression by 75.2% (n=4–5, P=0.0152) and 95.3% (n=3–4, P=0.0192), respectively (Fig. 5-A), and significantly decreased the EAG responses (by 36.9%) to all three ligands, E2HE2H (n=9, P=0.0112), E2HZ3H (n=9, P=0.0105), and E2HH (n=10, P=0.0406) (Fig. 5-B). Further behavior assays with the primary ligand showed that the males lost their preference for it (n=8, P=0.0257) (Fig. 5-C). No differences were observed between the non-injected and dsGFP control groups (Fig. 5-A and B), and no changes were detected in EAG responses to non-ligand plant odorants 2-phenylethanol and methyl salicylate (Fig. 5-B).

3.4. Homologs of OR23h and OR109d and their function validation

To differentiate the roles of RpedOR23h and RpedOR109d and identify additional ORs involved in aggregation pheromone perception, we conducted a phylogenetic analysis of RpedORs (>350 amino acids) alongside orthologs from four other hemipteran species. This revealed that RpedOR23h and RpedOR109d cluster into two distantly related lineages (Fig. 6-A). The RpedOR23h lineage included nine other RpedORs, while the RpedOR109d lineage included two other RpedORs (Fig. 6-A). We functionally characterized these 11

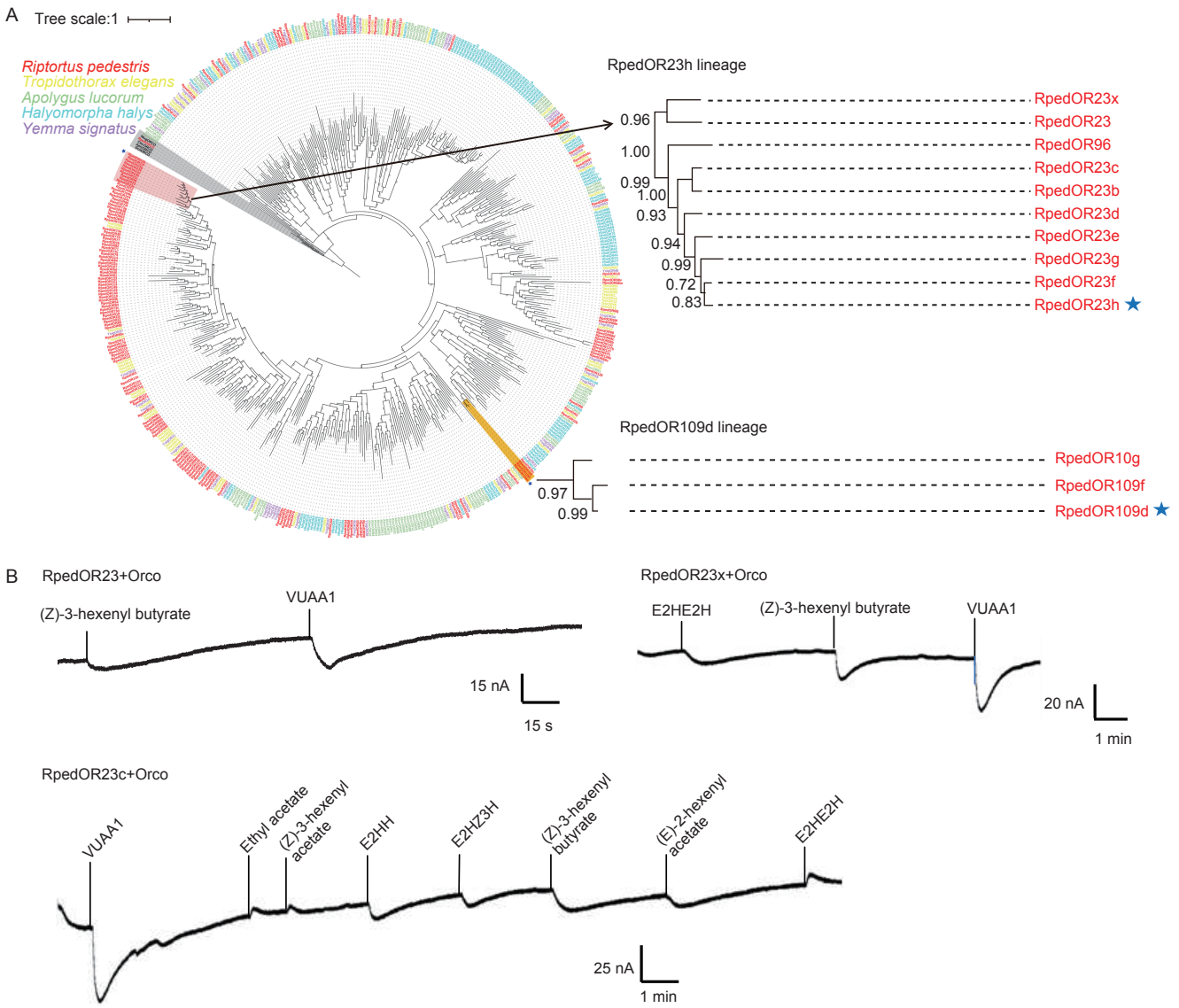

Fig. 6 Paralogs of RpedOR23h and RpedOR109d and their XOE-TEVC assay. A, the phylogenetic tree of *Riptortus pedestris* ORs and ORs of other Hemiptera insects, including *Halyomorpha halys* (Hhal), *Apolygus lucorum* (Aluc), *Yemma signatus* (Ysig), *Tropidothorax elegans* (Tele), *Diaphorina citri* (Dcit), *Cimex lectularius* (Clec), *Acyrthosiphon pisum* (Apis), and *Nilaparvata lugens* (Nlug). The tree was rooted with conserved Orco lineage (gray region). RpedOR23h and RpedOR109d are marked with blue stars. ORs of RpedOR23h lineage (pink region) and RpedOR109d lineage (orange region) are enlarged to the right. Numbers on nods indicate bootstrap values (only>70% are shown). B, current responses of RpedOR23, RpedOR23x, and RpedOR23c in XOE-TEVC assays with the ligand concentration of 5×10^{-4} mol L^{-1}.

homologs (excluding OR23f due to low antennal expression) using XOE-TEVC. Only three ORs in the RpedOR23h lineage (OR23x, OR23c and OR23) displayed a response to (*Z*)-3-hexenyl butyrate, a host plant odorant structurally similar to the three aggregation pheromones. In addition, OR23x was activated by E2HE2H, OR23c was activated by E2HZ3H and E2HH but inhibited by E2HE2H, while OR23 did not respond to any of the pheromone components (Fig. 6-B). No response was detected for the remaining seven homologs.

4. Discussion

Our study provides new insights into the molecular basis of aggregation pheromone perception in *R. pedestris*, offering an initial view of how phylogenetically distinct ORs with divergent ligand specificities and expression profiles may coordinate to decode chemical signals important for intraspecific communication. By integrating electrophysiology, transcriptomics, functional validation, and phylogenetic analysis, we identify key ORs involved in detecting aggregation pheromone components and suggest potential combinatorial coding strategies that contribute to behavioral responses to blended chemical cues.

Insects rely on specialized antennal segments to optimize chemical detection, with sensillum density and distribution often correlating with ecological needs (Hansson and Stensmyr 2011). Our finding that the antennal distiflagellum is the primary site for aggregation pheromone perception in *R. pedestris* aligns with morphological observations showing this segment contains twice as many sensilla as other antennal regions (Rani and Madhavendra 2005; Kim *et al.* 2016). Notably, the distiflagellum's role is not merely structural. Transcriptomic analysis revealed 197 ORs preferentially expressed in this segment, suggesting a transcriptional program tailored to pheromone detection. This contrasts with non-pheromonal olfactory tasks (e.g., host plant detection), which may rely on ORs distributed across other antennal regions. Such segment-specific OR expression reinforces the distiflagellum as a "pheromone-sensing hub," a specialization that likely evolved to prioritize detection of conspecific signals amid the chemical noise of the environment (Roh *et al.* 2021).

Our study uncovers the functional divergence between OR23h and OR109d, two ORs that underpin aggregation pheromone perception but exhibit striking differences in ligand tuning, expression, and phylogeny. OR23h acts as a "broadly tuned" receptor, responding to three structurally related pheromone components — E2HZ3H, E2HE2H, and E2HH — with the highest sensitivity to E2HZ3H. This broad tuning aligns with its expression across all life stages (adults and nymphs) and both sexes, suggesting it serves as a foundational detector for core aggregation signals. In contrast, OR109d is "narrowly tuned," responding exclusively to E2HE2H, and is expressed only in adult male antennae. This sex- and stage-specific expression implies a specialized role in male behavior, potentially linking E2HE2H to sexual communication — a hypothesis supported by earlier observations that E2HE2H abundance varies with mating status in males (Mizutani *et al.* 2008b).

The evolutionary significance of this divergence is notable. OR23h and OR109d cluster into distantly related phylogenetic lineages and share only 16.38% amino acid identity, indicating they likely evolved through independent adaptation. Such functional partitioning — where one receptor ensures broad detection of critical cues (OR23h) and another refines specificity for context-dependent signals (OR109d) — is a common strategy in insect olfaction, balancing robustness (to detect cues across variable conditions) and precision (to distinguish ecologically relevant signals) (Leal 2013; Sims *et al.* 2022). For *R. pedestris*, which encounters dynamic pheromone blends (e.g., varying with age, diet, or photoperiod; Huh *et al.* 2009), this division of labor may enhance behavioral flexibility: OR23h maintains baseline responsiveness to core components, while OR109d modulates male-specific responses to E2HE2H when needed.

Aggregation pheromones are typically blends of multiple components, and their behavioral efficacy often depends on cooperative detection by multiple receptors (Wertheim *et al.* 2006). Our results reveal a striking synergism between OR23h and OR109d in mediating E2HE2H perception in males: while silencing either receptor alone had minimal impact on EAG responses, dual silencing significantly reduced E2HE2H detection. This synergy is further supported by transcriptional upregulation of OR109d when OR23h is knocked down, suggesting a compensatory mechanism to maintain signal detection. Notably, OR109d's male-specific expression adds a sex-specific layer to this synergy. While both sexes exhibit similar EAG responses to E2HE2H, males may rely on OR109d to fine-tune responses (e.g., during mate searching), whereas females likely use other ORs for E2HE2H detection. This sexual dimorphism in receptor usage — without dimorphism in electrophysiological sensitivity — highlights the complexity of olfactory coding: behavioral responses emerge from the integration of receptor activity, not just individual receptor sensitivity.

We focused on four aggregation pheromone components that elicit EAG responses, but key questions remain about the fifth component, 18:iBu, and the functional roles of uncharacterized ORs. 18:iBu failed to induce detectable EAG responses in our assays, even at high dosages, which contrasts with field studies suggesting it may enhance attraction to 14:iBu (Yasuda *et al.* 2007a). This discrepancy raises the possibility that 18:iBu may act as a non-volatile, contact pheromone, detected *via* gustatory sensilla rather than antennal ORs. Similarly, ORs tuned to the core aggregation component 14:iBu — essential for congregation (Mizutani *et al.* 2007) — remain unknown. Given that 14:iBu is a long-chain ester structurally distinct from the other four components, its receptor may belong to a separate OR lineage. Future studies targeting distiflagellum-expressed ORs with low initial expression levels, or leveraging heterologous systems optimized for long-chain compound detection, may resolve this.

5. Conclusion

This study elucidates the dynamic perception of aggregation

pheromones in *R. pedestris*, orchestrated by the interplay between divergent odorant receptors. OR23h serves as a generalist receptor, ensuring detection of core pheromone components across life stages and sexes, while OR109d acts as a male-specific specialist, refining responses to E2HE2H. Their synergistic interaction ensures reliable detection of critical blends, balancing robustness and precision in a variable chemical environment. These insights not only advance our understanding of insect olfactory coding but also provide a roadmap for developing targeted pest control strategies — ultimately bridging molecular mechanisms to applied entomology. Future work will focus on identifying ORs for 14:iBu and 18:iBu, exploring central nervous system integration of OR signals, and testing whether OR-targeted compounds can enhance trap efficacy in field settings. By unraveling this network, we move closer to decoding the chemical language of *R. pedestris* and leveraging it for sustainable pest management.

Acknowledgements

This work was supported by grants from the National Key Research and Development Program of China (2023YFD1401000) and the National Natural Science Foundation of China (32372530). We thank Pherobio Technology Co., Ltd., China for providing the chemical E2HZ3H used in this study.

Declaration of competing interest

The authors declare that they have no conflict of interest.

Declaration of generative AI and AI-assisted technologies in the writing process

During the preparation of this manuscript, the authors used DeepSeek-V3 to assist with translation of some draft content and to improve the clarity and readability of the language. All content generated was carefully reviewed and revised by the authors as necessary, and the authors take full responsibility for the final content of the article.

Ethical statements

All applicable international, national and institutional guidelines for the care and use of animals were followed.

Appendices associated with this paper are available at https://doi.org/10.1016/j.jia.2025.11.009

References

Endo N, Takashi W, Nobuo M, Seiichi M, Rikiya S. 2005. Ambiguous response of *Riptortus clavatus* (Heteroptera: Alydidae) to different blends of its aggregation pheromone components. *Applied Entomology and Zoology*, **40**, 41–45.

Guo J M, Wei Z Q, Hou J H, He Y, Luan X P, Zhang Y Y, Liu X L, Zhang X T, Zhang J, Yan Q, Dong S L. 2023. Ionotropic receptor IR75q.2 mediates avoidance reaction to nonanoic acid in the fall armyworm *Spodoptera frugiperda* (Lepidoptera, Noctuidae). *Journal of Agricultural and Food Chemistry*, **71**, 20602–20612.

Guo X J, He H, Sun J H, Kang L. 2023. Plasticity of aggregation pheromones in insects. *Current Opinion in Insect Science*, **59**, 101098.

Guo X J, Yu Q Q, Chen D F, Wei J N, Yang P C, Yu J, Wang X H, Kang L. 2020. 4-vinylanisole is an aggregation pheromone in locusts. *Nature*, **584**, 584–588.

Hallem E A, Carlson J R. 2006. Coding of odors by a receptor repertoire. *Cell*, **125**, 143–160.

Hallem E A, Dahanukar A, Carlson J R. 2006. Insect odor and taste receptors. *Annual Review of Entomology*, **51**, 113–135.

Hansson B S, Stensmyr M C. 2011. Evolution of insect olfaction. *Neuron*, **72**, 698–711.

Huh H S, Jang S A, Park C G. 2009. Variation in aggregation pheromone secretion of bean bug, *Riptortus clavatus*. *Korean Journal of Applied Entomology*, **48**, 1612–1617.

Huh H S, Park K H, Seo W D, Park C G. 2005. Interaction of aggregation pheromone components of the bean bug, *Riptortus clavatus* (Thunberg) (Heteroptera: Alydidae). *Applied Entomology and Zoology*, **40**, 643–648.

Huh W, Park C G. 2010. Effect of day length and temperature on the diapause termination of *Riptortus pedestris* (Hemiptera: Alydidae) male adults. *Korean Journal of Applied Entomology*, **49**, 205–210.

Karlson P, Lüscher M. 1959. 'Pheromones': A new term for a class of biologically active substances. *Nature*, **183**, 55–56.

Kim J, Park K C, Roh H S, Kim J, Oh H W, Kim J A, Park C G. 2016. Morphology and distribution of antennal sensilla of the bean bug *Riptortus pedestris* (Hemiptera: Alydidae). *Microscopy Research and Technique*, **79**, 501–511.

Kong H L, Guo D, Zhang L, Xie D J, Wilson K, Jiang X F. 2025. Enhanced immune responses of gregarious larvae contribute to successful adult migration in the migratory oriental armyworm. *Journal of Integrative Agriculture*, **24**, 3141–3154.

Leal W S. 2013. Odorant reception in insects: Roles of receptors, binding proteins, and degrading enzymes. *Annual Review of Entomology*, **58**, 373–391.

Leal W S, Higuchi H, Mizutani N, Nakamori H, Kadosawa T, Ono M. 1995. Multifunctional communication in *Riptortus clavatus* (Heteroptera: Alydidae): Conspecific nymphs and egg parasitoid *Ooencyrtus nezarae* use the same adult attractant pheromone as chemical cue. *Journal of Chemical Ecology*, **21**, 973–985.

Leal W S, Kadosawa T. 1992. (*E*)-2-hexenyl hexanoate, the alarm pheromone of the bean bug *Riptortus clavatus* (Heteroptera: Alydidae). *Bioscience, Biotechnology, and Biochemistry*, **56**, 1004–1005.

Liu X L, Zhang J, Yan Q, Miao C L, Han W K, Hou W, Yang K, Hansson B S, Peng Y C, Guo J M, Xu H, Wang C Z, Dong S L, Knaden M. 2020. The molecular basis of host selection in a crucifer-specialized moth. *Current Biology*, **30**, 4476–4482.e5.

Liu W, Cai C, Wu J, Wang B. 2025. A pheromone from cuticular hydrocarbons regulates mating behavior in the hoverfly *Eupeodes corollae*. *Journal of Integrative Agriculture*, **24**, 4732–4743.

Love M I, Huber W, Anders S. 2014. Moderated estimation of fold change and dispersion for RNA-Seq data with DESeq2. *Genome Biology*, **15**, 550.

Mizutani N, Wada T, Higuchi H, Ono M, Leal W S. 1997. A component of a synthetic aggregation pheromone of *Riptortus clavatus* (THUNBERG) (Heteroptera: Alydidae), that attracts an egg parasitoid, *Ooencyrtus nezarae* ISHII (Hymenoptera: Encyrtidae). *Applied Entomology and Zoology*, **32**, 504–507.

Mizutani N, Wada T, Yasuda T, Endo N, Yamaguchi T, Moriya S. 2008a. Influence of photoperiod on attractiveness and pheromone contents of the bean bug, *Riptortus pedestris* (Heteroptera: Alydidae). *Applied Entomology and Zoology*, **43**, 585–592.

Mizutani N, Yasuda T, Yamaguchi T, Moriya S. 2007. Individual variation in the amounts of pheromone components in the male bean bug, *Riptortus pedestris* (Heteroptera: Alydidae) and its attractiveness to the same species. *Applied Entomology and Zoology*, **42**, 629–636.

Mizutani N, Yasuda T, Yamaguchi T, Moriya S. 2008b. Pheromone contents and physiological conditions of adult bean bugs, *Riptortus pedestris* (Heteroptera: Alydidae), attracted to conspecific males during non-diapause and diapause periods in fields. *Applied Entomology and Zoology*, **43**, 331–339.

Morishima M, Tabuchi K, Ito K, Mizutani N, Moriya S. 2005. Effect of feeding on the attractiveness of *Riptortus clavatus* (Thunberg) (Heteroptera: Alydidae) males to conspecific individuals. *Japanese Journal of Applied Entomology and Zoology*, **49**, 262–265.

Numata H, Kon M, Hidaka T. 1990. Male adults attract conspecific adults in the bean bug, *Riptortus clavatus* THUNBERG: Heteroptera: Alydidae. *Applied Entomology and Zoology*, **25**, 144–145.

Rahman M M, Lim U T. 2017. Evaluation of aggregation and alarm pheromones of *Riptortus pedestris* (Hemiptera: Alydidae) as a push–pull strategy in soybean fields. *Applied Entomology and Zoology*, **52**, 469–479.

Rahman M M, Kim E, Kim D, Bhuyain M M, Lim U T. 2018. Use of aggregation pheromone traps increases infestation of adult *Riptortus pedestris* (Hemiptera: Alydidae) in soybean fields. *Pest Management Science*, **74**, 2578–2588.

Rani P U, Madhavendra S S. 2005. External morphology of antennal and rostral sensillae in four hemipteran insects and their possible role in host plant selection. *International Journal of Tropical Insect Science*, **25**, 198–207.

Roh G H, Cha D H, Park C G. 2021. Olfactory attraction to aggregation pheromone is mediated by disti-flagellum of antennal segments in *Riptortus pedestris*. *Journal of Asia-Pacific Entomology*, **24**, 415–420.

Sims C, Birkett M A, Withall D M. 2022. Enantiomeric discrimination in insects: The role of OBPs and ORs. *Insects*, **13**, 368.

Sun D D, Zhang Y T, Cao S, Wang X Q, Cao Q, Zhang S, Liu Y. 2025. A compound produced by *Helicoverpa armigera* male genitalia activates a conserved pheromone receptor. *Journal of Integrative Agriculture*, **24**, 1892–1904.

Tabuchi K, Moriya S, Mizutani N. 2005. Seasonal catches of the bean bug, *Riptortus clavatus* (Thunberg) (Heteroptera: Alydidae), in water-pan traps with synthetic attractants. *Japanese Journal of Applied Entomology and Zoology*, **49**, 99–104.

Tateishi K, Nishimura Y, Sakuma M, Yokohari F, Watanabe H. 2020. Sensory neurons that respond to sex and aggregation pheromones in the nymphal cockroach. *Scientific Reports*, **10**, 1995.

Vickers N J. 2017. Animal communication: When I'm calling you, will you answer too? *Current Biology*, **27**, R713–R715.

Wertheim B, Allemand R, Vet L E M, Dicke M. 2006. Effects of aggregation pheromone on individual behaviour and food web interactions: A field study on *Drosophila*. *Ecological Entomology*, **31**, 216–226.

Wertheim B, Baalen E J A V, Dicke M, Vet L E M. 2005. Pheromone-mediated aggregation in nonsocial arthropods: An evolutionary ecological perspective. *Annual Review of Entomology*, **50**, 321–346.

Yasuda T, Mizutani N, Endo N, Fukuda T, Matsuyama T, Ito K, Moriya S, Sasaki R. 2007a. A new component of attractive aggregation pheromone in the bean bug, *Riptortus clavatus* (Thunberg) (Heteroptera: Alydidae). *Applied Entomology and Zoology*, **42**, 1–7.

Yasuda T, Mizutani N, Honda Y, Endo N, Yamaguchi T, Moriya S, Fukuda T, Sasaki R. 2007b. A supplemental component of aggregation attractant pheromone in the bean bug *Riptortus clavatus* (Thunberg) (Heteroptera: Alydidae), related to food exploitation. *Applied Entomology and Zoology*, **42**, 161–166.

Yew J Y, Chung H. 2015. Insect pheromones: An overview of function, form, and discovery. *Progress in Lipid Research*, **59**, 88–105.

Yuvaraj J K, Roberts R E, Sonntag Y, Hou X Q, Grosse-Wilde E, Machara A, Zhang D D, Hansson B S, Johanson U, Löfstedt C, Andersson M N. 2021. Putative ligand binding sites of two functionally characterized bark beetle odorant receptors. *BMC Biology*, **19**, 16.

Zhang X T, Luan X P, Wei J H, Zhang P P, Guo J M, Keesey I W, Gao Y, Yan Q, Zhang J, Dong S L. 2024. Identification of a soybean volatile attractive for *Riptortus pedestris* using reverse chemical ecology approach. *Journal of Agricultural and Food Chemistry*, **72**, 27084–27093.